

# Solid Phase and Solution Phase Structural Characterization of Pyrene-Based, T-Shaped Molecular Dyads

Donocadh P. Lydon,<sup>[a]</sup> Peiyi Li,<sup>[a]</sup> Andrew C. Benniston,<sup>\*[a]</sup> William McFarlane,<sup>[b]</sup>  
Ross W. Harrington,<sup>[c]</sup> and William Clegg<sup>[c]</sup>

**Keywords:** Pyrene / Spiropyran / Isomerization

Structural solid-phase and solution-phase properties of two pyrene-spiropyran molecular dyads are described. Each dyad comprises a 1,1'-[indole-4,6-diylbis(ethyne-2,1-diyl)]-bis(pyrene) backbone, with the bis(pyrene) and spiropyran units adopting a T-shaped arrangement. The strength of the C<sub>spiro</sub>-O bond is altered by replacement of H by NO<sub>2</sub> in the terminal aryl group of the spiropyran unit. X-ray crystal structure determinations carried out for two of the dyads (H and NO<sub>2</sub>) reveal the pyrene groups to be aligned *anti* to each other. The crystal packing diagrams are different; both con-

tain pyrene  $\pi$ -stacked centro-symmetric dimers, but in one structure this is the total extent of the  $\pi$  stacking whereas the other structure has pyrene dimers interleaved to generate infinite parallel stacks. Detailed <sup>1</sup>H NOE experiments are consistent with a solution-phase structure that differs markedly from the solid-state structure, and in which the pyrene groups are *syn* to one another but orientated away from the spiropyran group.

(© Wiley-VCH Verlag GmbH & Co. KGaA, 69451 Weinheim, Germany, 2007)

## Introduction

The many factors that combine to control the dynamics of electron-transfer processes have been unravelled and explained over the preceding decades, and there now exists a profound theoretical understanding of such reactions.<sup>[1]</sup> Attention is now focussed on how to exploit this knowledge to design advanced molecular-scale devices and machines.<sup>[2]</sup> Several important practical applications of electron-transfer phenomena have emerged in recent years and cover such diverse fields as chemical sensors,<sup>[3]</sup> light-emitting diodes<sup>[4]</sup> molecular rectifiers,<sup>[5]</sup> artificial enzymes<sup>[6]</sup> and signal transduction.<sup>[7]</sup> Future goals include the development of effective mimics of the natural photosynthetic light-harvesting complex,<sup>[8]</sup> and the design of miniaturized opto-electronic components.<sup>[9]</sup> These latter systems either use light or create light by way of coupled charge-transfer processes and are intended to offset the increasing demand for high speed and high efficiency processing, transmission, and reception of information. Whilst it is clear that there is no requirement to replace all the components present in a conventional

electronic circuit with molecular-scale analogues, it is certain that the new circuitry will need to replicate key features of current integrated circuits. In particular, it is essential that circuit-breakers and molecular-scale switches become available in the near future.<sup>[10]</sup>

The design of a molecular T-junction, whereby electronic information can be directed along orthogonal pathways, presents a formidable challenge to contemporary science.<sup>[11]</sup> This task is greatly amplified if the two pathways are to be topologically equivalent. Promising routes towards the development of fast optical switches involve systems capable of large-scale torsional motion under illumination<sup>[12]</sup> and many such photochromic materials have been reported.<sup>[13–15]</sup> Related approaches use stimulated translational motion to re-position molecular units along linear chains. Again, numerous such rotaxanes and catenanes have been devised in recent years.<sup>[16]</sup> None of these systems, however, can be used as the scaffold for a molecular T-junction.

In a recent report we described the synthesis and spectroscopy of two molecular systems that incorporate the necessary overall T-shaped arrangement (Figure 1).<sup>[17]</sup> Selective light activation of the pyrene unit leads to ring opening of the spiropyran to afford the merocyanine form (MC). Creation of the MC form extends the  $\pi$  conjugation from the central phenylene ring and thus introduces a new chromophore into the T-junction. We were able to elucidate the mechanism for spiropyran ring opening in PY-SPN occurred via an intramolecular exciplex which can be formulated as PY<sup>-</sup> NMe<sup>+</sup>. For efficient exciplex formation it is reasonable to assume that a close proximity of the pyrene to the spiropyran tertiary nitrogen is warranted. Clearly

[a] Molecular Photonics Laboratory, School of Natural Sciences, Newcastle University, Newcastle NE1 7RU, United Kingdom  
Fax: +44-191-222-6929  
E-mail: a.c.benniston@ncl.ac.uk

[b] NMR Spectroscopy Centre, School of Natural Sciences, Newcastle University, Newcastle NE1 7RU, United Kingdom

[c] Crystallography Laboratory, School of Natural Sciences, Newcastle University, Newcastle NE1 7RU, United Kingdom

Supporting information for this article is available on the WWW under <http://www.eurjoc.org> or from the author.

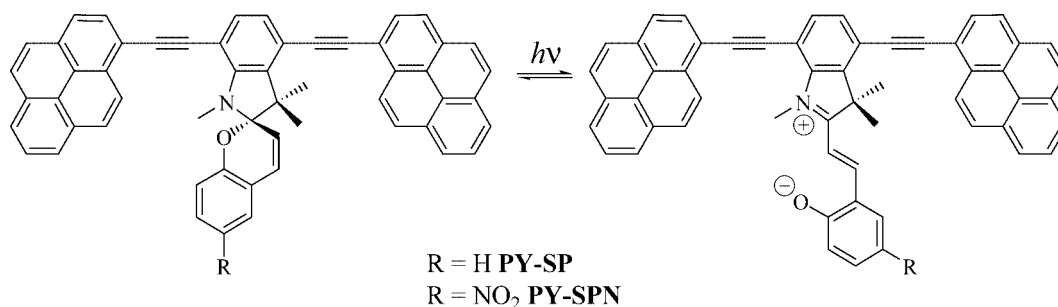


Figure 1. Illustration of the two T-shaped dyads discussed herein.

from the substitution pattern of the pyrene unit, rotation can dispose the unit away from the spiropyran group. One would expect the rotation process to be relatively facile in fluid solution but more restricted in a glass or the solid phase. Because ultimately we expected to use the T-shaped dyads in an organized medium for Write-Read-Erase<sup>[18]</sup> applications, a more comprehensive structural study was required. Here, we describe the solid-state structures and low-temperature structural studies for the two dyads in an attempt to elucidate their rotamer distribution.

## Results and Discussion

The synthesis of **PY-SP** and **PY-SPN** has been described previously,<sup>[17]</sup> but a detailed analysis of their solid- and solution-phase structures was not given. Hence, to ascertain the ground-state structure for the T-shaped relays, **PY-SP** and **PY-SPN** were subjected to single-crystal, X-ray crystallographic studies. This was complemented by detailed NMR analysis on **PY-SPN**, to ascertain the relative positioning of the pyrene units with respect to the spiropyran group. Illustrated in Figure 2 are views of the molecular structures for **PY-SP** and **PY-SPN**, and collected in Table 1 are selected bond lengths and angles. The first point to note, for both structures, is the relative positioning of the pyrene subunits. The pyrene groups are essentially coplanar (with dihedral angles of 3.8 and 3.1° for **PY-SP** and **PY-SPN**, respectively) and lie *anti* to each other, with one being displaced away from the *gem*-dimethyl groups of the spiropyran unit. This is presumably due to steric reasons and to facilitate crystal packing. In each case, the pyrene groups are twisted somewhat out of the plane of the benzene ring that lies between them, the twist being somewhat larger for **PY-SPN** (dihedral angles 22.6 and 24.6°, compared with 10.1 and 13.9° for **PY-SP**). The closest contact distance between the nitrogen of the spiropyran and the pyrene group N1–C52 are 5.293 Å and 5.047 Å for **PY-SPN** and **PY-SP**, respectively. Also important to note is the increase in the C–O bond length for the spiro segment on replacing H by NO<sub>2</sub> in the terminal aryl ring. This alteration is accompanied by a decrease in the pyramidal nature of the *N*-methyl site in the indolene unit, as measured by the sum of bond angles at the N atom (Table 1). Aldoshin<sup>[19]</sup> has proposed that an interaction takes place between the nitrogen lone pair and the *anti*-bonding  $\sigma^*$ -or-

bital for the C<sub>spiro</sub>–O bond, which accounts for the lengthening of the C<sub>spiro</sub>–O bond. Thus, the increase in C<sub>spiro</sub>–O bond length for **PY-SPN** is a result of the electron-withdrawing nitro group weakening that bond. It should be noted that the spiro carbon labeled C1 is a chiral center; the synthetic procedure is such that both enantiomers are produced in a racemic mixture; the crystal structures are centro-symmetric.

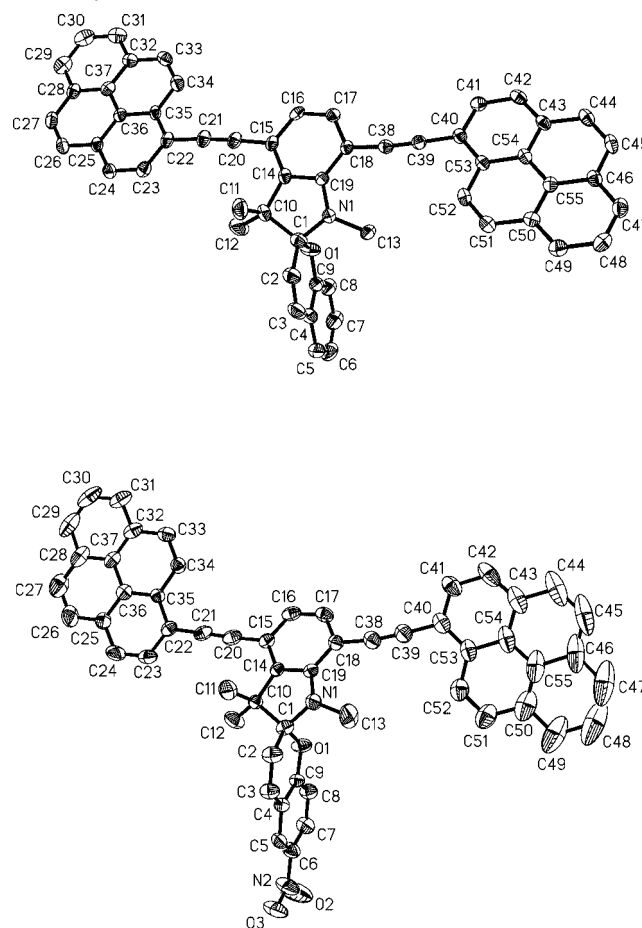


Figure 2. Ellipsoid representations (50% probability level) of the molecular structures for T-shaped compounds **PY-SP** (top) and **PY-SPN** (bottom). Atomic numbering is shown and hydrogen atoms are omitted for clarity.

Despite the obvious molecular similarity between **PY-SP** and **PY-SPN**, the crystal packings for the two are disparate (Figure 3), which is not surprising because one is a chloro-

Table 1. Selected bond lengths and angles for **PY-SP** and **PY-SPN**.

Bond lengths [Å]/angles [°]	<b>PY-SP</b>	<b>PY-SPN</b>
C1–N1	1.464(3)	1.476(5)
C13–N1	1.465(3)	1.458(5)
C19–N1	1.416(3)	1.404(4)
C1–O1	1.467(3)	1.507(4)
C1–C2	1.503(4)	1.469(5)
O1–C1–N1	106.4(2)	104.6(3)
O1–C1–C2	112.7(2)	111.8(3)
O1–C1–C10	105.1(2)	106.6(2)
Sum of angles at N1	343.5	350.8

form solvate and the other a toluene solvate. For both molecules, centro-symmetric dimers are formed in which pyrene units are stacked essentially parallel to each other with a separation of about 3.4 Å, indicating intermolecular  $\pi$ -stacking interactions, as is common for pyrene derivatives.<sup>[20]</sup> In the case of **PY-SPN**, overlap of the pyrene units, when viewed normal to their planes, is rather small and the dimers are arranged in such a way that stacking does not continue beyond the dimer. In the crystal structure of **PY-**

**SP**, however, there is greater overlap of the pyrene units and the dimers are interleaved so as to form continuous stacks running parallel throughout the structure.

### <sup>1</sup>H NMR Structural Characterization

The dissimilar crystal-packing features for the two dyads are an indication that their structures might be significantly different in solid and solution phases. That rotation of the pyrene units may take place in fluid solution leads to four planar conformations (Figure 4), that differ in the relative orientations of the two pyrene units. First, the two pyrene groups can be on the same side and point either towards or away from the spiropyran unit (conformers **1** and **4**). Second, two *anti* arrangements are feasible that depend on whether or not a pyrene points towards or away from the *N*-methyl group of the spiropyran (conformers **2** and **3**). Clearly, conformations are also possible where the pyrene groups are not coplanar with the spiropyran moiety, though extended  $\pi$  conjugation is reduced in such rotamers. As indicated from structural determinations, the pyrene groups can approach within ca. 5 Å of the *N*-methyl and *gem*-dimethyl groups of the spiropyran (f, g and h) as well as the two protons (i, j) of the indolene unit. This distance is within the range that might be expected to give Nuclear Overhauser Enhancement (NOE)<sup>[21]</sup> effects for protons associated with the indolene and pyrene groups. With this in mind, the most probable NOE's for each conformation are illustrated by arrows in Figure 4. The unique NOE patterns for each of the conformers (**1–4**) facilitates their identification. However, in order to carry out this task specific proton assignments for **PY-SPN** are required.

### Proton Peak Assignment

Assignment of specific proton resonances associated with the pyrene and spiropyran residues was performed using a number of routine NMR spectroscopic techniques (for supporting information see also the footnote on the first page of this paper). The main complication is unequivocal identification of resonances associated with protons 2 and 10 for each pyrene unit, because there is substantial overlap of signals in the aromatic region. Identification of other proton signals was more straightforward and listed in Table 2 are selected proton shifts and assignments.

The singlet peak at  $\delta = 1.42$  ppm with an integral of 3H is identified as the methyl group, g, on the basis of a cross correlation with the alkenyl proton, e, using ROESY. The peak at  $\delta = 1.71$  ppm, again with an integral of 3H, is thus assigned to methyl group, f, because it displays a cross-correlation peak in the ROESY with the methyl group g. Because of its characteristic chemical shift and integral, the peak at  $\delta = 3.45$  ppm is readily assigned to the methyl group marked k. Owing to the identical coupling constants ( $J = 10.4$  Hz) and TOCSY correlation, the two doublets at  $\delta = 5.88$  and 6.98 ppm are identified as the alkenyl protons e and d. That only the proton signal at  $\delta = 5.88$  ppm displays

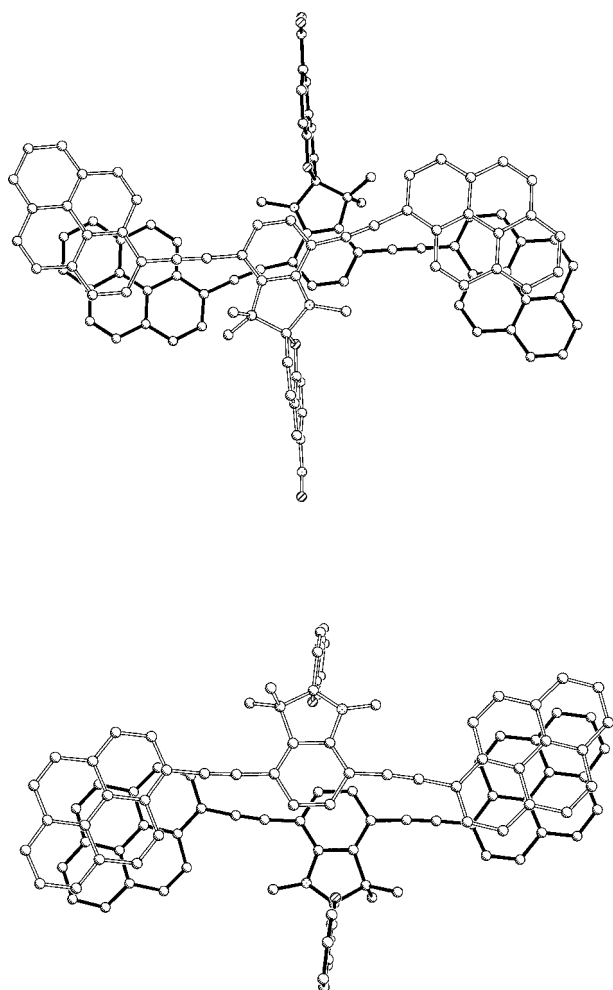


Figure 3.  $\pi$ -Stacked centrosymmetric dimers for **PY-SPN** (top) and **PY-SP** (bottom); hydrogen atoms are omitted for clarity.

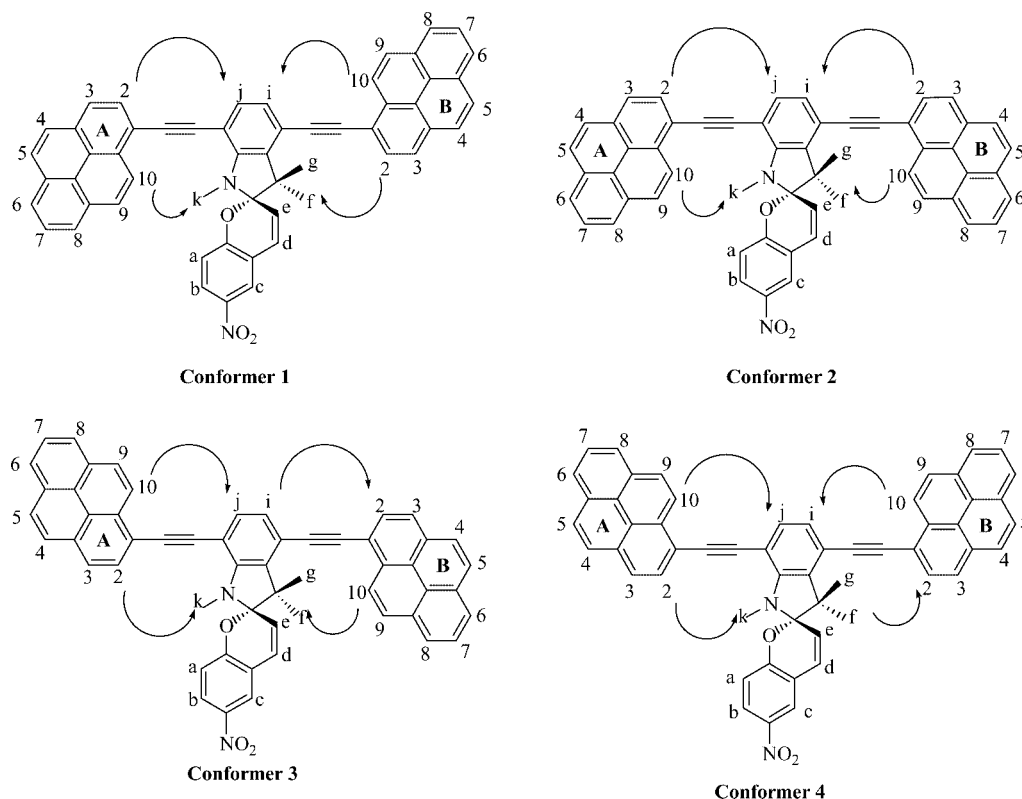


Figure 4. Illustrations of the four possible planar conformers for **PY-SPN** in fluid solution, and the corresponding proton numbering and lettering Scheme. Arrows depict the most significant NOE's expected between proton pairs that could be used for conformer assignment.

Table 2. Selected  $^1\text{H}$  and  $^{13}\text{C}$  NMR shifts and assignments for **PY-SPN** in  $\text{CD}_2\text{Cl}_2$ .<sup>[a]</sup>

Site	$\delta$ ( $^1\text{H}$ ) ppm <sup>[b]</sup>	$\delta$ ( $^{13}\text{C}$ ) ppm <sup>[b]</sup>
A	6.84	115.85
B	7.98	123.18
C	8.07	129.34
D	6.98	129.48
E	5.88	121.36
F	1.71	20.29
G	1.42	23.80
i	7.21	124.61
j	7.53	133.52
k	3.45	31.71
A2	8.09	—
A7/B7	7.97	—
A9	8.11	—
A10	8.55	125.66
B2	8.15	—
B9	8.10	—
B10	8.60	125.66

[a] Solvent signal used as the internal reference. [b]  $\pm 0.01$  ppm.

a strong NOE to the methyl group, g, unequivocally assigns this signal to the proton marked e.

Verification of proton signals for i and j rely on assigning signals for a and b, because these two protons could have shown, to a first approximation, similar coupling patterns. However, the signal at  $\delta = 6.84$  ppm is readily assigned to proton a because of its ROESY correlations with protons k and f but not g. Assignments of proton resonances for b and c at  $\delta = 7.98$  and  $8.07$  ppm, respectively, are now

straightforward using a combination of TOCSY<sup>[21]</sup> and ROESY<sup>[21]</sup> experiments and by acquiring a *J*-resolved spectrum (Table 2). Hence, the two doublets at  $\delta = 7.21$  and  $7.53$  ppm are assigned to protons i and j, respectively owing to the similar coupling constants ( $J = 7.95$  Hz) and cross-correlations in the TOCSY spectrum.

The two doublets at  $\delta = 8.55$  and  $8.60$  ppm are identified as protons, 10, for the two pyrene rings due to their characteristic chemical shifts (compare 1-fluoropyrene and other 1-substituted pyrene derivatives). Both these signals show cross-correlation to resonances buried in the multiplet associated with the remaining pyrene signals. Deconvolution of all the overlapping proton resonances for the multiplet was not possible, and only a limited number of resonances can be assigned (Table 2). However, the doublet resonances at  $\delta = 8.09$  and  $8.15$  ppm could be assigned to the pyrene protons, 2, because of cross-correlations with f and g in the ROESY spectra. The triplet identified from the *J*-resolved spectrum at  $\delta = 7.97$  ppm is due to proton 7, although this proton is too remote to display significant NOE's to protons associated with the spiropyran residue. The same argument can be invoked for the remaining pyrene protons.

### Solution Stereochemistry

The ROESY spectrum recorded for **PY-SPN** at room temperature in  $\text{CD}_2\text{Cl}_2$  shows far fewer long-range NOE's than the one collected at  $-70^\circ\text{C}$ . One implication for such



behavior is that at room temperature there is considerable conformational mobility and relatively free pyrene rotation on the NMR time scale. In contrast, at the lower temperature there is a degree of dominance by just a few rotamers.

Commencing at conformer **1**, which corresponds to the solid-state structure, it is reasonable to expect that the NOE between proton pair **B10** and **i** would be much stronger than the corresponding NOE between **A10** and **j**. Because this is not the case, conformer **1** can be discounted as the dominant rotamer in solution. Similar reasoning can be used to discount conformer **3**. That experimentally the proton pair interaction between **A10** and **j** is much stronger than for the proton pair **A2** and **i** rules out conformer **2** as a major rotamer. This result seems reasonable, since for this conformer there will exist a high level of steric crowding between **A10** and **k** and between **B10** and **f**, **g**. These deductions leave only conformer **4** as the major rotamer in solution. The ROESY experiments reveal a strong NOE between proton pair **A10** and **j**, as well as between protons **B10** and **i**. Other NOE interactions are observed between proton pairs **B2** and **f**, and **A2** and **k**. Both these results are fully consistent with the proposed conformer assignment. Rather surprisingly there are also interactions between protons **A10** and **k**, and between protons **B10** and **f**. At first sight, these results seem contradictory and are more in fitting with an assignment to conformers **1** and **2**. However, when comparing the different conformers one has to take into account the difference in distances between proton pairs and the  $r^{-6}$  NOE distance dependence.<sup>[21]</sup> The **A10** to **k** distance in conformers **1** and **2** is some 20% shorter than the **A2** to **k** distance for conformers **3** and **4**, leading to a factor of almost three for the NOE's. Thus, the NOE interaction in the former case would be expected to be much stronger than that observed experimentally, so the apparent inconsistency is illusory. Similar considerations apply to the **B10** interactions. It is worth noting that NOE interaction is also observed between proton pair **j** and **k** though they are quite remote in all conformers.<sup>[22]</sup>

The foregoing analysis ignores possible contributions from conformers in which the pyrene groups are not coplanar with the central benzenoid ring. If such contributions were large this would represent an approach to "free rotation" leading to a reduction in the differences in the NOE's noted above. That is, they may well be significant at higher temperatures, but are probably relatively minor at  $-70\text{ }^{\circ}\text{C}$ .

## Conclusions

Considering the similarity in structure of the asymmetric unit in the solid state for **PY-SPN** and **PY-SP** it is reasonable to assume that their solution phase structures will be very similar. The lowest-energy conformer appears, at least at low temperature in fluid solution, to arrange the pyrene groups away from the spiropyran moiety. By comparison,  $\pi$  stacking of the pyrene units appears to dominate when the dyads are allowed to form organised structures. Clearly some aspect of the rotamer problem can be solved by mov-

ing the substitution position in the pyrene to the 1-position so that only perpendicular structures need to be considered. Future work is underway to create new T-shaped dyads where exciplex formation is enhanced to facilitate ring opening and molecular ordering is better controlled in the solid state. This later feature is one we hope to exploit in the generation of solid state Write-Read-Erase devices.

## Experimental Section

Compounds were made as described previously and purified.<sup>[17]</sup> Several different NMR experiments were carried out on **PY-SPN** in  $\text{CD}_2\text{Cl}_2$  using a Jeol Lambda spectrometer operating at 500.16 MHz for protons and 125.26 MHz for  $^{13}\text{C}$  using standard pulse sequences. Proton 2-D TOCSY spectra were recorded at  $20\text{ }^{\circ}\text{C}$  with a 25 ms mixing time; this experiment is equivalent to short-range COSY. Proton 2-D J-resolved NMR spectra were recorded at  $24\text{ }^{\circ}\text{C}$  to aid assignments in congested parts of the aromatic region of the spectra.  $^1\text{H}$  2-D ROESY spectra were collected at  $-70\text{ }^{\circ}\text{C}$  with a 250 ms mixing time and an initial  $2\text{ K} \times 0.5\text{ K}$  data matrix **S2** which was zero-filled to  $2\text{ K} \times 2\text{ K}$  prior to processing. Indirect detected H/C correlation spectra (HSQC) and long-range H/C correlations spectra (HMBC) for the aromatic region, with timings optimized for  $^3J$  ( $^{13}\text{C}$ -H) interactions, were all recorded at  $24\text{ }^{\circ}\text{C}$ .

Crystals suitable for X-ray diffraction were obtained by slow evaporation of solutions of **PY-SP** in  $\text{CHCl}_3$  or **PY-SPN** in toluene. Details pertaining to the two structural determinations are collected in Table 3. Data were collected on a Nonius KappaCCD dif-

Table 3. X-ray crystallographic data and refinement parameters for spiropyran derivatives.

	PY-SP	PY-SPN
Molecular formula	$\text{C}_{56}\text{H}_{36}\text{Cl}_3\text{NO}$	$\text{C}_{61}\text{H}_{42}\text{N}_2\text{O}_3$
<i>M</i>	845.2	851.0
<i>a</i> [Å]	11.254(6)	9.8842(14)
<i>b</i> [Å]	11.822(6)	13.869(2)
<i>c</i> [Å]	16.514(6)	17.558(2)
$\gamma$ [°]	80.43(3)	89.983(13)
<i>V</i> [Å <sup>3</sup> ]	2081.9(17)	2246.0(6)
$\alpha$ [°]	81.36(4)	69.735(12)
$\beta$ [°]	75.27(3)	84.483(11)
$\gamma$ [°]	80.43(3)	89.983(13)
<i>Z</i>	2	2
<i>D</i> <sub>calcd.</sub> [g cm <sup>-3</sup> ]	1.348	1.258
Crystal system	triclinic	triclinic
Space group	<i>P</i> $\bar{1}$	<i>P</i> $\bar{1}$
Diffractometer	Nonius Kappa-CCD	Nonius Kappa-CCD
Radiation, $\lambda$ [Å]	Mo- <i>K</i> $\alpha$ , 0.71073	Mo- <i>K</i> $\alpha$ , 0.71073
Crystal size [mm]	$0.20 \times 0.10 \times 0.10$	$0.40 \times 0.12 \times 0.10$
<i>T</i> [K]	150	150
$\theta$ range [°]	4.0 to 24.0	4.1 to 22.5
Reflections measured	32980	24273
Independent reflections	6479	5812
<i>R</i> <sub>int</sub>	0.0641	0.0423
Reflections with $F^2 > 2\sigma$	4347	4044
Absorption coeff. [mm <sup>-1</sup> ]	0.264	0.077
Max./min. transmission	0.950/0.975	0.970/0.992
<i>R</i> [ <i>F</i> , $F^2 > 2\sigma$ ]	0.0546	0.0837
<i>R</i> <sub>w</sub> [ $F^2$ , all data]	0.1179	0.2607
<i>S</i> [ $F^2$ , all data]	1.062	1.068
Refined parameters	553	546
Max./min. electron density [e Å <sup>-3</sup> ]	0.22/−0.31	0.82/−0.42

fractometer, and corrected semi-empirically for absorption, based on repeated and symmetry-equivalent reflections. The structures were solved by direct methods and refined on all  $F^2$  values. Chloroform solvent could be modeled with discrete atoms in one structure, but highly disordered toluene in the other structure had to be treated with the SQUEEZE procedure of PLATON (A. L. Spek, University of Utrecht, The Netherlands). Other programs were standard Nonius control and integration software, and Bruker SHELXTL.

CCDC-631378 and -631379 contain the supplementary crystallographic data for this paper. These data can be obtained free of charge from The Cambridge Crystallographic Data Centre via [www.ccdc.cam.ac.uk/data\\_request/cif](http://www.ccdc.cam.ac.uk/data_request/cif).

**Supporting Information** (see also the footnote on the first page of this article): Four figures (S1–S4) showing the crystal packing views for **PY-SPN** and **PY-SP**, the full-range cross-correlated ROESY spectrum recorded for **PY-SPN** in  $\text{CD}_2\text{Cl}_2$  at  $-70^\circ\text{C}$ , and individual cross-sections from the ROESY spectrum recorded for **PY-SPN** in  $\text{CD}_2\text{Cl}_2$  at  $-70^\circ\text{C}$  (two figures for the latter).

## Acknowledgments

We thank Engineering and Physical Sciences Research Council (EPSRC) (EP/C007727), the Leverhulme Trust (F/00125/J) and the University of Newcastle for financial support.

- [1] a) J.-L. Brédas, D. Beljonne, V. Coropceanu, J. Cornil, *Chem. Rev.* **2004**, *104*, 4971–5003; b) J. T. Hupp, R. D. Williams, *Acc. Chem. Res.* **2001**, *34*, 808–817; c) R. A. Marcus, *Angew. Chem. Int. Ed. Engl.* **1993**, *32*, 1111–1121.
- [2] a) M. J. Blanco, M. C. Jimenez, J.-C. Chambron, V. Heitz, M. Linke, J.-P. Sauvage, *Chem. Soc. Rev.* **1999**, *28*, 293–305; b) V. Balzani, A. Credi, F. M. Raymo, J. F. Stoddart, *Angew. Chem. Int. Ed.* **2000**, *39*, 3349–3391; c) A. P. de Silva, N. D. McClenaghan, *Chem. Eur. J.* **2004**, *10*, 574–586; d) A. Credi, B. Ferrer, *Pure Appl. Chem.* **2005**, *77*, 1051–1057.
- [3] a) M. H. Keefe, K. D. Benkstein, J. T. Hupp, *Coord. Chem. Rev.* **2000**, *205*, 201–228; b) S. S. Sun, A. J. Lees, *Coord. Chem. Rev.* **2002**, *230*, 171–192; c) A. P. de Silva, B. McCaughan, B. O. F. McKinnery, M. Querol, *Dalton Trans.* **2003**, 1902–1913.
- [4] J. L. Bredas, D. Beljonne, V. Coropceanu, J. Cornil, *Chem. Rev.* **2004**, *104*, 4971–5003.
- [5] R. M. Metzger, *Anal. Chim. Acta* **2006**, *568*, 146–155.
- [6] I. Willner, B. Willner, *Top. Curr. Chem.* **1991**, *159*, 153–218.
- [7] a) M. Inouye, K. Akamatsu, H. Nakazumi, *J. Am. Chem. Soc.* **1997**, *119*, 9160–9165; b) S. D. Wettig, G. A. Bare, R. J. S. Skinner, J. S. Lee, *Nano Lett.* **2003**, *3*, 617–622.
- [8] a) J. S. Hsiao, B. P. Krueger, R. W. Wagner, T. E. Johnson, J. K. Delaney, D. C. Mauzerall, G. R. Fleming, J. S. Lindsey, D. F. Bocian, R. J. Donohoe, *J. Am. Chem. Soc.* **1996**, *118*, 11181–11193; b) T. S. Balaban, A. Eichhofer, J.-M. Lehn, *Eur. J. Org. Chem.* **2000**, *24*, 4047–4057.
- [9] D. Holton, D. F. Bocian, J. S. Lindsey, *Acc. Chem. Res.* **2002**, *35*, 57–69.
- [10] F. M. Raymo, M. Tomasulo, *Chem. Soc. Rev.* **2005**, *34*, 327–336.
- [11] A. C. Benniston, *Chem. Soc. Rev.* **2004**, *33*, 573–578.
- [12] A. C. Benniston, A. Harriman, *Angew. Chem. Int. Ed. Engl.* **1993**, *32*, 1459–1461.
- [13] G. H. Brown (Eds.), *Techniques of Chemistry*, vol. III, *Photochromism*, Wiley Interscience, **1971**.
- [14] V. I. Minkin, *Chem. Rev.* **2004**, *104*, 2751–2776.
- [15] a) H. Bouas-Laurent, H. Dürr, *Pure Appl. Chem.* **2001**, *73*, 639–665; b) B. L. Feringa, W. F. Jager, B. de Lange, *Tetrahedron* **1993**, *49*, 8267–8310.
- [16] a) A. C. Benniston, A. Harriman, V. M. Lynch, *J. Am. Chem. Soc.* **1995**, *117*, 5275–5291; b) M. Murakami, A. Kawabuchi, K. Kato, M. Kunitake, N. Nakashima, *J. Am. Chem. Soc.* **1997**, *119*, 7605–7606.
- [17] A. C. Benniston, A. Harriman, S. L. Howell, P. Li, D. P. Lydon, *J. Org. Chem.* **2007**, *72*, 888–897.
- [18] J.-M. Lehn, *Supramolecular Chemistry: Concepts and Perspectives*, Wiley-VCH, Weinheim, **1995**.
- [19] S. M. Aldoshin, L. A. Nikonova, V. A. Smirnov, G. V. Shilov, N. K. Nagaeva, *J. Mol. Struct.* **2005**, *750*, 158–165.
- [20] a) J. M. Robertson, J. G. White, *J. Chem. Soc.* **1947**, 358–368; b) R. Ziessel, C. Goze, G. Ulrich, M. Césario, P. Retailleau, A. Harriman, J. P. Rostron, *Chem. Eur. J.* **2005**, *11*, 7366–7378.
- [21] J. K. M. Sanders, B. K. Hunter, in *Modern NMR Spectroscopy, A Guide for Chemists*, 2nd ed., Oxford University Press, **1993**.
- [22] The correlation may also be long range coupling which is sometimes observed with 500 MHz measurements.

Received: December 19, 2006

Published Online: February 13, 2007